Multiscale approach to modeling intrinsic dissipation in solids

K. Kunal and N. R. Aluru

A multi-scale approach to model intrinsic dissipation in solids.

K. Kunal and N. R. Aluru*

Department of Mechanical Science and Engineering,

Beckman Institute for Advanced Science and Technology,

University of Illinois at Urbana-Champaign, Urbana, IL 61801

(Dated: July 19, 2016)

Abstract

In this work, we develop a multi-scale approach to model intrinsic dissipation under high frequency of vibrations in solids. For vibrations with time-scale comparable to the phonon relaxation time, the local phonon distribution deviates from the equilibrium distribution. We extend the quasi-harmonic (QHM) method to describe the dynamics under such a condition. The local deviation from the equilibrium state is characterized using a non-equilibrium stress tensor. A constitutive relation for the time evolution of the stress component is obtained. We, then, parametrize the evolution equation using the QHM method and a stochastic sampling approach. The stress relaxation dynamics is obtained using mode Langevin dynamics. Methods to obtain the input variables for the Langevin dynamics are discussed. The proposed methodology is used to obtain the dissipation rate, E_{dissip}, for different cases. Frequency and size effect on E_{dissip} are studied. The results are compared with those obtained using non-equilibrium molecular dynamics (MD).

I. INTRODUCTION

High frequency vibrations in nano electro mechanical systems (NEMS) have importance for a wide variety of technological applications and for the fundamental understanding of physical phenomenon. Technological relevance include atomic scale mass sensors[1,2], detection of biological molecules[3–5] and the detection of electron spin flip[6] as few select examples. From a fundamental perspective nano-resonators have been devised to probe physical phenomenon such as non-linear dynamics[7] and quantum effects in macroscopic objects[8]. An important aspect for all these applications is dissipation in NEMS which limits its performance. For example, observing quantum effects in a macroscopic sized object requires that the device is in the quantum ground state. For an oscillator this necessitates that $h\omega_n >> k_b T$. Here, h is the Planck's constant, ω_n is the angular frequency, k_b is the Boltzmann constant and T is the temperature. This explains the need for high values of ω_n. However, dissipation or coupling with the environment leads to thermalization and smears out the quantum effect. A low dissipation rate is, therefore, desired.

Modeling of dissipation at the nano-scale is, therefore, of central importance for design of NEMS devices. Depending on the medium that exchanges energy with the motion of interest, the dissipation mechanisms can be broadly classified as the extrinsic and the intrinsic mechanisms. Extrinsic dissipation[10–15] involves the loss of mechanical energy because of coupling with the external environment while intrinsic damping results from energy exchange with the internal thermal vibration of the structure. Extrinsic damping can often be minimized using better design considerations. Intrinsic energy loss, however, sets a fundamental limit for the device performance. The different known mechanisms of intrinsic dissipation include thermo-elastic damping[16,17] (TED), Akhiezer damping[18–20], non-linear coupling between mechanical modes[21–24], surface mediated losses[25,26] and dissipation due to defects[27–29].

Intrinsic dissipation takes place as a result of the coupling between the mechanical deformation and the internal thermal vibrations in a structure. An irreversible flow of energy takes place resulting in an increase in the entropy of the system. In the classical thermo-elasticity the thermal vibrations are quantified in terms of the temperature field. Such a description invokes the condition of local equilibrium. The mean thermal energy or the temperature field, then, suffices as a complete description of the system. However, this

approximation is not valid in the case of nano-resonators.

Nano-resonators have vibrational frequency in the order of few GHz. For such high frequencies of vibration the time-scale of mechanical deformation becomes comparable to the phonon relaxation time. Deformation of a structure, at rates comparable to the phonon relaxation time, drives the phonon out of equilibrium. For such cases the mean thermal energy or the temperature is not an adequate description of the thermal field. Additional variables, that characterize the deviation from equilibrium, are required to describe the thermal field. The out of equilibrium phonon population, then, results in the absorption of energy from the mechanical deformation. Akhiezer mechanism[30] characterizes the damping due to this local disturbance of the phonon population. The dissipation rate due to the Akhiezer mechanism is, often, quantified using a reduced order two oscillator model[31]. In this work, we provide a detailed quasi-harmonic based multi-scale approach to model intrinsic dissipation due to perturbation of the local phonon distribution. The time-scale for the thermalization of phonons is generally of the order of few ps. In the frequency space this corresponds to a frequency range of 1-100 GHZ. Hence, the dissipation due to local phonon perturbation is expected to play an important role in nano-resonators. This provides a motivation for this study. However, other dissipation mechanisms may also play an important role. The relative contribution of other damping processes needs to be analyzed and each of it merits a study of its own.

The thermal vibrations in a structure and its coupling with the mechanical field are described using the quasi-harmonic (QHM) method[32,33]. The existing QHM frame-work is, however, valid for quasi-static deformation. In this work we extend the QHM method to model the intrinsic dissipation in solids under the high frequency vibrations. We introduce a non-equilibrium component of the stress tensor, $\boldsymbol{\sigma}'$. The stress tensor characterizes the deviation from local equilibrium and vanishes under quasi-static deformation. A constitutive relation that governs the time evolution of $\boldsymbol{\sigma}'$ is obtained. The time evolution for $\boldsymbol{\sigma}'$ is described by a forcing and a relaxation term. The forcing rate is parametrized in terms of a dissipation tensor $\mathbf{D}$ which is obtained using QHM. We, also discuss a stochastic sampling method to obtain $\mathbf{D}$. The relaxation dynamics for $\boldsymbol{\sigma}'$ is obtained using Langevin dynamics in the basis of normal modes. In this approach each of the modes is modeled as a noisy harmonic oscillator. The proposed methodology is, then, used to study the effect of different parameters on the dissipation rate. Vibrations with frequency in the range of few GHz are

considered. The results are compared with those obtained using non-equilibrium MD.

The manuscript is organized as follows. In section II we obtain the constitutive relation for σ' using QHM. Methods to obtain the dissipation tensor, $\mathbf{D}$, and the stress relaxation rates are, then, discussed. In section III we apply the method to compute the dissipation rate as a function of different parameters. The comparisons with the MD results are provided alongside. Finally, the conclusions are given in section IV.

II. THEORY AND METHODS

In this section we will first obtain an expression for the non-equilibrium stress using the quasi harmonic (QHM) method. We will then derive a constitutive relation that governs the time evolution of the non-equilibrium stress. The constitutive relation, as obtained, shows two physical processes a forcing term and a relaxation term. The forcing term will be characterized in terms of a dissipation tensor $\mathbf{D}$. An expression for $\mathbf{D}$ in terms of the material parameters will be obtained. We will also discuss a non-equilibrium sampling method to parametrize $\mathbf{D}$. We will, then, describe the stress relaxation behavior. Langevin dynamics and Green Kubo formulation will be used in this regard.

A. Non-Equilibrium Stress

In this section we shall derive an expression for stress tensor under non-equilibrium condition. We consider the case of a crystalline structure that is amenable to the quasi-harmonic approximation. This implies that the atoms undergo small thermal vibrations about the mean positions. For a given mean position of atoms, the quasi-harmonic approximation then suffices to describe the thermal vibrations. We briefly describe the QHM method. For the details of QHM the reader is referred to[32,33]. In essence the QHM method considers a Taylor series expansion of the governing inter-atomic potential for a given mean position of the atoms. The potential energy is, then, approximated by retaining the second order terms in the expansion. The quadratic expression for the truncated Hamiltonian is decoupled using normal modes. These normal modes constitute a set of orthogonal directions in the configuration space. For the quadratic Hamiltonian, the motion along one direction is independent along the other. It should be mentioned that the normal modes are a function

4

of the mean atomic position (or strain) in QHM. The dependence of modes on strain, indeed, gives the coupling between the strain and the thermal vibrations. A harmonic method, for which the eigen-vector and the frequencies are invariant under deformation, cannot describe dissipation.

Using QHM the Hamiltonian, can, thus, be written in terms of the modal co-ordinates. Let a_i denote the mode displacement, ω_i denote the frequency and v_i be the velocity for a mode i. The Hamiltonian, H, is, given as

$$H = \sum_{i=1}^{nmodes} \frac{1}{2}m\omega_i^2 a_i^2 + \frac{1}{2}mv_i^2. \tag{1}$$

Here, $nmodes$ is the number of modes and m is the atomic mass. $nmodes = 3 \times nat$, where nat is the number of atoms in the system.

The thermal state of the system is completely described by specifying the probability density function (PDF) for the mode co-ordinates. Under the equilibrium condition, characterized by temperature, T, the PDF for a_i is given as

$$P(a_i) = \frac{1}{Z}exp\left(-\frac{m\omega_i^2 a_i^2}{2k_bT}\right) \tag{2}$$

Here, k_b is the Boltzmann constant and Z is the partition function.

The PDF in Eq.(2) is only valid under the condition of local equilibrium. When this condition is violated, the modes no longer satisfy the energy equipartition principle. Instead each mode i is characterized by a non-equilibrium temperature T_i. The PDF, $P_{neqb}(a_i)$, for a_i for such a state is, then, given as

$$P_{neqb}(a_i) = \frac{1}{Z}exp\left(-\frac{m\omega_i^2 a_i^2}{2k_bT_i}\right) \tag{3}$$

This expression for $P_{neqb}(a_i)$ has been obtained using the principle of maximum entropy[34]. A derivation for this is provided in Appendix A. In deriving the above expression, the phonon distribution is considered to have a temperature different from the ambient. The assumption holds only under the condition of weak coupling with the environment. Under a more general condition, the mean temperature of phonons will tend to relax towards the ambient value. For such cases, additional equations that describe this relaxation dynamics, will be required. In this work we have neglected the coupling with the environment.

We, shall, now derive an expression for the stress tensor for the non-equilibrium state.

Let $\boldsymbol{\sigma}$ denote the thermal stress tensor and let σ_{ij} denote its components. σ_{ij} is given as

$$\sigma_{ij} = \frac{1}{V}\frac{\partial <H>}{\partial \epsilon_{ij}} \tag{4}$$

Here, and for all future purpose, the symbol $<...>$ refers to the ensemble average. V is the volume and ϵ_{ij} are the components of the strain tensor, $\boldsymbol{\epsilon}$. Using the expression for H in Eq.(1) and the PDF in Eq.(3), we obtain

$$\sigma_{ij} = \frac{1}{V}\sum_{n=1}^{nmodes}\int \frac{1}{2}m\frac{\partial \omega_n^2}{\partial \epsilon_{ij}}a_n^2 P(a_n)da_n \tag{5}$$

We define λ_n^{ij} such that $\lambda_n^{ij} = \frac{1}{\omega_n}\frac{\partial \omega_n}{\partial \epsilon_{ij}}$. Using the definition of λ_n^{ij} and further simplifying Eq.(5) we get

$$\sigma_{ij} = \frac{1}{V}\sum_{n=1}^{nmodes}\lambda_n^{ij}E_n. \tag{6}$$

Here, E_n is the mean energy for mode n and is related to T_n as $E_n = k_bT_n$. Using a little algebra, the expression for σ_{ij} can be, further, re-casted as

$$\sigma_{ij} = \frac{nmodes}{V}\overline{\lambda^{ij}}\,\overline{E} + \frac{1}{V}\sum_{n=1}^{nmodes}\Delta\lambda_n^{ij}\Delta E_n \tag{7}$$

Here, and for all future reference, the symbol $\overline{x}$ is defined as $\overline{x} = \frac{1}{nmodes}\sum_{n=1}^{nmodes}x_n$, where x_n is any mode variable for mode n. Also, $\Delta E_n = E_n - \overline{E}$ and $\Delta\lambda_n^{ij} = \lambda_n^{ij} - \overline{\lambda^{ij}}$. We have, thus, decomposed the stress into two components. Under the condition of equilibrium, the modes satisfy the energy equi-partition principle and we have $\Delta E_n = 0$. The second term in Eq.(7), then, vanishes. We, thus, identify this term as the non-equilibrium component of the stress tensor, $\boldsymbol{\sigma}'$. While the equilibrium stress is a state property, the non-equilibrium stress depends on the rate of deformation of the system. In the next section we will derive an Eq. that governs the time evolution of $\boldsymbol{\sigma}'$. The components of $\boldsymbol{\sigma}'$ are, therefore, given as

$$\sigma_{ij}' = \frac{1}{V}\sum_{n=1}^{nmodes}\Delta\lambda_n^{ij}\Delta E_n \tag{8}$$

B. Constitutive Relation

In this section we will derive the constitutive relation that governs the time evolution of $\boldsymbol{\sigma}'$. Using physical arguments we first state the result. We shall, then, provide a derivation for the different terms in the expression based on the QHM method. We will also present

a non-equilibrium sampling approach to parametrize the constitutive relation in the next section.

The time evolution of $\boldsymbol{\sigma}'$ is given as

$$\frac{d\boldsymbol{\sigma}'}{dt} = \mathbf{D}\frac{\partial \boldsymbol{\epsilon}}{\partial t} + \left(\frac{\partial \boldsymbol{\sigma}'}{\partial t}\right)_{relax} \tag{9}$$

Here, $\mathbf{D}$ is a fourth order dissipation tensor and the second term on the R.H.S describes the relaxation of the stress tensor. An expression for $\mathbf{D}$ will be derived subsequently. Eq.(9) shows that the evolution of $\boldsymbol{\sigma}'$ results from two competing factors. Deformation of the system at any finite rate drives it out of equilibrium. Under the linear approximation, the rate at which the system deviates from the equilibrium state is proportional to the driving rate. The first term in the above Eq. describes this phenomenon. Further, if left unperturbed, the system tends to relax towards the corresponding equilibrium state. $\boldsymbol{\sigma}'$, which measures the deviation from the equilibrium state, correspondingly relaxes towards a zero value. This is described by the second term in Eq.(9).

In-order to derive the Eq. that governs the time evolution of $\boldsymbol{\sigma}'$ we take the derivative of Eq.(8) with respect to time. We, then, obtain

$$\dot{\sigma}'_{ij} = \frac{1}{V}\sum_{n=1}^{nmodes}\Delta\lambda_n^{ij}\Delta\dot{E}_n \tag{10}$$

In the above Eq. we need to substitute the time derivative of ΔE_n. The energy of a mode changes due to two processes. The applied deformation field injects (or extracts) energy from each of the modes. Further, the modes interact with each other and an inter-modal flow of energy takes place. We shall first consider the energy change due to the applied strain. The partial change in E_n due to the change in strain, ϵ_{ij}, is obtained as

$$\frac{\partial E_n}{\partial \epsilon_{ij}} = \int \frac{1}{2}m\frac{\partial \omega_n^2}{\partial \epsilon_{ij}}a_n^2 P_{neqb}(a_n)da_n \tag{11}$$

Using the expression for $P_{neqb}(a_n)$ in Eq.(3) and carrying out the integration we obtain

$$\left(\frac{\partial E_n}{\partial t}\right)_{\epsilon_{ij}} = \lambda_n^{ij}E_n\frac{d\epsilon_{ij}}{dt} \tag{12}$$

Here, $\left(\frac{\partial E_n}{\partial t}\right)_{\epsilon_{ij}}$ denotes the time rate of change of E_n due to the change in ϵ_{ij}.

Adding the above Eq. for all values of n we obtain

$$\left(\frac{\partial \overline{E}}{\partial t}\right)_{\epsilon_{ij}} = \overline{\lambda^{ij}}\,\overline{E}\frac{d\epsilon_{ij}}{dt} + \overline{\Delta\lambda^{ij}\Delta E}\frac{d\epsilon_{ij}}{dt} \tag{13}$$

7

Here, $\left(\frac{\partial \overline{E}}{\partial t}\right)_{\epsilon_{ij}}$ denotes the time rate of change of $\overline{E}$ due to the change in ϵ_{ij}. For small deformations in the linear regime, the system shows a weak deviation from the equilibrium state. Under such a condition, the second term in the RHS of Eq.(13) is negligible in comparison with the first term. Neglecting the second order terms and taking the difference between Eq.(13) and Eq.(12) we get

$$\left(\frac{\partial \Delta E_n}{\partial t}\right)_{\epsilon_{ij}} = \Delta\lambda_n^{ij} k_b T \frac{d\epsilon_{ij}}{dt} \tag{14}$$

Here, $\left(\frac{\partial \Delta E_n}{\partial t}\right)_{\epsilon_{ij}}$ denotes the time rate of change of ΔE_n due to the change in ϵ_{ij}. In deriving the above expression we have also used the approximation that $E_n \approx k_b T$. We have, thus, obtained an expression for the time rate of change of ΔE_n due to the change in ϵ_{ij}. We will now discuss the case of inter-modal interaction.

Let $\left(\frac{\partial \Delta E_n}{\partial t}\right)_{coll}$ denote the time rate of change of ΔE_n due to inter modal interaction. Using a single relaxation time approximation this is, often, given as $\left(\frac{\partial \Delta E_n}{\partial t}\right)_{coll} = -\frac{\Delta E_n}{\tau}$. Here, τ denotes the single relaxation time for all the modes. We will, however, not use the single relaxation time approximation. Instead, we shall resort to mode Langevin dynamics and obtain an effective relaxation rate for $\boldsymbol{\sigma}'$. In this approach, each mode n has its own characteristic relaxation time τ_n. The details of stress relaxation will be discussed in the later section. For the time being we shall just retain the expression $\left(\frac{\partial \Delta E_n}{\partial t}\right)_{coll}$ to denote the energy change due to collision.

The total rate of change of ΔE_n due to strain and the inter-modal interaction is, then, obtained as

$$\frac{d\Delta E_n}{dt} = k_b T \Delta\lambda_n^{ij} \frac{d\epsilon_{ij}}{dt} + \left(\frac{\partial \Delta E_n}{\partial t}\right)_{coll} \tag{15}$$

Using this expression in Eq.(10) we obtain

$$\frac{d\sigma_{ij}'}{dt} = \frac{1}{V}\left[\sum_{p=1,q=1}^{3,3}\sum_{n=1}^{nmodes} k_b T \Delta\lambda_n^{ij} \Delta\lambda_n^{pq} \frac{d\epsilon_{pq}}{dt} + \sum_{n=1}^{nmodes}\left(\frac{\partial \Delta\lambda_n^{ij} \Delta E_n}{\partial t}\right)_{coll}\right] \tag{16}$$

In-order to write the above Eq. in a compact form we define the fourth order dissipation tensor $\mathbf{D}$. The components of $\mathbf{D}$ are given as

$$D_{ijkl} = \frac{3k_b T \rho}{m}\overline{\Delta\lambda_n^{ij} \Delta\lambda_n^{kl}} \tag{17}$$

Here, ρ is density and m is the atomic mass. We realize that the second term in Eq.(16) denotes the relaxation of the non-equilibrium stress. Eq.(16) can, therefore, be re-casted as

$$\frac{d\boldsymbol{\sigma}'}{dt} = \mathbf{D}\frac{\partial \boldsymbol{\epsilon}}{\partial t} + \left(\frac{\partial \boldsymbol{\sigma}'}{\partial t}\right)_{relax} \tag{18}$$

8

We, thus, obtain a constitutive relation that governs the time evolution of $\boldsymbol{\sigma}'$. The dissipation tensor, $\mathbf{D}$, can be obtained from QHM using Eq.(17) . It, still, remains to parametrize the relaxation term in the governing Eq. and this will be pursued in the latter section. Before discussing the relaxation dynamics we will discuss an alternative approach to parametrize $\mathbf{D}$. In this approach a stochastic method is used to sample the non-equilibrium states.

C. Non-Equilibrium Stochastic Sampling

In the previous section, the QHM approximation was used to obtain an expression for the non-equilibrium stress tensor, $\boldsymbol{\sigma}'$. Subsequently, we derived an expression for the time evolution of $\boldsymbol{\sigma}'$. We obtained a dissipation tensor, $\mathbf{D}$ that characterizes the time rate of change of $\boldsymbol{\sigma}'$ due to the change in $\boldsymbol{\epsilon}$. We can, alternatively, obtain $\mathbf{D}$ by measuring the stress for a system as a function of its deviation from the equilibrium state. In this approach, we use virial stress tensor obtained using the inter-atomic potential. The QHM approximation for the stress, as used in the previous section, is not invoked. In-order to motivate this approach we shall, first, provide a physical interpretation of $\mathbf{D}$.

We consider a system that is initially in thermal equilibrium and is subjected to a differential strain $d\epsilon_{ij}$. Let $d\sigma_{ij}^{V}$ denote the differential change in the virial component of stress and as measured instantaneously. The term instantaneous, here, implies time scales which are small compared with the time required for thermalization. $d\sigma_{ij}^{V}$, then, results from two processes. First, it results from the change in the mean position of the atoms and corresponds to the elastic contribution. Secondly, it results from the system being driven out of the equilibrium state and corresponds to the dissipative component. Let $d\sigma_{ij}^{D}$ denote the component of σ_{ij}^{V} that results from the second effect. The dissipation tensor $\mathbf{D}$ can, then, be obtained such that its components are given as

$$D_{ijkl} = \frac{\partial \sigma_{ij}^{D}}{\partial \epsilon_{kl}} \tag{19}$$

We, will, use the above Eq. to compute D_{ijkl}. For this purpose, we need to extract the stress component that results from the deviation of the system from the equilibrium state. In-order to obtain this, we will generate atomic configurations in the non-equilibrium state and with the same mean position of the atoms. The difference in the stress value of the

9

non-equilibrium state from the equilibrium configurations, then, gives us σ_{ij}^D. Stochastic sampling approach will be used for this purpose. In essence, the stochastic sampling approach generates the micro-states according to a given PDF. For computing $\mathbf{D}$ we use a non-equilibrium PDF. Hence, the method is referred to as non-equilibrium stochastic sampling. We will briefly outline the approach here. The details of the algorithm, for performing the stochastic sampling, is discussed in Appendix B.

For sampling a non-equilibrium state we, first, need to characterize it and construct the corresponding PDF. We construct the PDF in the basis of the mode co-ordinates. We consider a non-equilibrium state that results from applying an instantaneous strain ϵ_{kl} on the system. This results in a different change in the frequency of different modes and hence having different temperature. For a mode i, the change in temperature, ΔT_i, is related to the change in the potential energy, ΔPE_i, as $\Delta T_i = \frac{\Delta PE_i}{2k_b}$. Further, ΔPE_i can be approximated as $\Delta PE_i = \frac{1}{2}m\frac{\partial \omega_i^2}{\partial \epsilon_{kl}} < a_i^2 > \epsilon_{kl}$. Using the relation, $\lambda_i^{kl} = \frac{\partial \omega_i}{\omega_i \partial \epsilon_{kl}}$ we get $\Delta T_i = T_0(1 + \lambda_i^{kl}\epsilon_{kl})$. Here T_0 is the temperature in the initial state. Let T be the mean temperature for the final strained state and is obtained as $T = T_0(1 + \overline{\lambda_i^{kl}}\epsilon_{kl})$. T_i can then be expressed as $T_i = T + \Delta\lambda_i^{kl}\epsilon_{kl}T_0$. The different terms have the same representation as introduced before. The PDF for a_i is, then, obtained, as

$$P(a_i) = \frac{1}{Z}exp\left(-\frac{m\omega_i^2 a_i^2}{k_b T_i}\right) \tag{20}$$

For a given value of ϵ_{kl} we, first, determine the values of T_i for all the modes. The PDF for a_i is, then, constructed, using Eq.(20). We sample the values of a_i using the given PDF. The a_i values are used to determine the atomic displacement using the linear transformation. An atomic configuration is, thus, obtained. Different samples are generated in this manner. The sampled sets are, then, used to compute the virial stress tensor. Let σ_{ij}^V denote the mean virial stress tensor for a given non-equilibrium state. We also determine σ_{ij}^V for the equilibrium configuration. The difference between the two values gives the dissipative stress σ_{ij}^D. From the slope of the linear fit of σ_{ij}^D vs ϵ_{kl}, D_{ijkl} is determined.

D.   Stress Relaxation

The constitutive relation for the time evolution of $\boldsymbol{\sigma}'$ in Eq.(9) has two governing terms. The first term on the R.H.S corresponds to the forcing term while the second one describes

the relaxation towards equilibrium. The forcing term was characterized using $\mathbf{D}$. We have, already, discussed methods to obtain $\mathbf{D}$ in the previous sections. In this section we seek to characterize the relaxation behavior of the non-equilibrium stress component.

Microscopically, stress relaxation results from the interaction between the different modes. We, therefore, need to model the modal dynamics to characterize this behavior. We will use the Langevin frame-work to describe the dynamics of the modes. Further, we shall resort to the Green-Kubo formulation and obtain the stress relaxation. For the systems considered, the stress relaxation shows an exponentially decaying behavior. We will, therefore, eventually characterize the relaxation of $\boldsymbol{\sigma}'$ using an effective relaxation rate, τ_{relax}, such that

$$\left(\frac{\partial \boldsymbol{\sigma}'}{\partial t}\right)_{relax} = -\frac{\boldsymbol{\sigma}'}{\tau_{relax}} \tag{21}$$

The objective of this section is to provide an algorithm to determine τ_{relax} for different structures. It would be useful, here, to briefly outline the main steps in the algorithm. This will aid the reader in understanding the general flow of the section. We will use mode Langevin dynamics to determine τ_{relax}. The first step required for the Langevin simulation is the parametrization. Langevin simulation needs as an input the momentum relaxation time, τ_i^m, for mode i. We shall use a stochastic sampling approach to determine τ_i^m. For determining τ_i^m using the stochastic sampling approach, one needs an additional information of the noise relaxation time, τ_i^n. This closure is provided by performing a MD simulation of a reference bulk structure. The τ_i^m values are, then, used to perform the Langevin simulation and determine τ_{relax}.

The section is organized as follows. We will, first, state the governing Eq. for the mode Langevin dynamics and describe the different input parameters. We will, then, discuss the method to determine τ_i^n using MD for a bulk reference structure. Next, we shall discuss the stochastic sampling approach to determine the momentum relaxation time τ_i^m. This completes the discussion on parametrization step. Finally, the method to determine τ_{relax} using the mode Langevin dynamics will be discussed.

1. Langevin Dynamics

The Eq. governing the dynamics of a mode i, using the Langevin approximation, is given as

$$m\frac{d^2 a_i}{dt^2} + \frac{2m}{\tau_i^m}v_i + m\omega_i^2 a_i = r_i(t) \tag{22}$$

Here, m is the effective mass, ω_i is the mode frequency and τ_i^m is the momentum relaxation time. r_i is the noise force with a correlation time τ_i^n such that $r_i(0)r_i(t) =< r_i^2 > exp(-t/\tau_i^n)$. For the cases considered, τ_i^n is of the order of few fs. Hence, the Langevin approximation suffices for describing the mode dynamics. Further, τ_i^n, τ_i^m and r_i are related using the fluctuation dissipation theorem as

$$< r_i^2 >= \frac{2mk_b T}{\tau_i^n \tau_i^m} \tag{23}$$

This relation will be used in the parametrization step. For evolving Eq.(22) we need to know the values of different terms. The mode frequency, ω_i, is obtained using the QHM method. We first use bulk MD as a parametrization step to determine τ_i^n.

We consider a bulk structure with a dimension of 8 unit cells in each direction. The structure is first equilibrated at a desired temperature using the Nosé-Hoover thermostat. It is, then, evolved as a micro-canonical ensemble. The generated trajectories are used to determine the time series data of the mode variables. We, thus, obtain the mode displacement, $a_i(t)$, the mode velocity, $v_i(t)$, and the mode force, $f_i(t)$ as a function of time.

We construct the velocity auto-correlation function (VACF), $C_{v_i v_i}(t)$, such that

$$C_{v_i v_i}(t) =< v_i(0)v_i(t) > . \tag{24}$$

VACF shows an oscillatory decaying behavior. From the decay rate, the momentum relaxation time, τ_i^m, is determined for the bulk structure. We need to determine the value of τ_i^n. For determining τ_i^n, we first equate the MD modal force with the mode force from the Langevin model. We, thus, obtain

$$f_i(t) = -m\omega_i^2 a_i(t) - \frac{2mv_i(t)}{\tau_i^m} + r_i(t) \tag{25}$$

Further, rearranging the above Eq. and taking the second moment of the L.H.S and the R.H.S we get

$$< (f_i + m\omega_i^2 a_i)^2 >=< \left(\frac{2mv_i}{\tau_i^m}\right)^2 > + < r_i^2 > \tag{26}$$

In deriving this expression we used the condition that $< f_i v_i >= 0$. This indeed is true for the equilibrium state. Further, using $< v_i^2 >= \frac{k_b T}{m}$ and the relation in Eq.(23) we obtain

$$< (f_i + m\omega_i^2 a_i)^2 >= \frac{4mk_b T}{(\tau_i^m)^2} + \frac{2mk_b T}{\tau_i^n \tau_i^m} \qquad (27)$$

The L.H.S of the above Eq. can be computed using the time series data of mode variables $f_i(t)$ and $a_i(t)$. These are obtained from the bulk MD simulation. τ_i^m was determined using the VACF as discussed before. These values are, then, substituted in Eq.(27) to determine τ_i^n. We compute τ_i^n for different modes. Figure 1 shows the noise relaxation time obtained using MD for a bulk nickel structure. A strong dependence of τ_i^n on ω_i is observed. We perform a polynomial fit of τ_i^n vs. ω_i using the data set obtained. The fitted function is the first step in the parametrization for Langevin simulation. This information will now be used to determine the τ_i^m values of any other structure of interest.
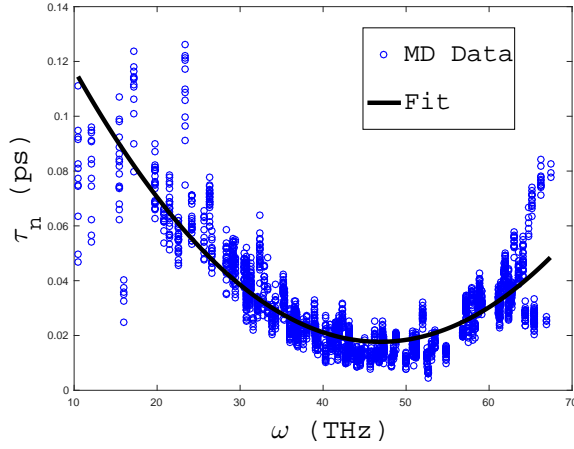

FIG. 1. Noise relaxation time as a function of mode frequency obtained using MD. The polynomial fit is, also, shown.

We consider the case of a structure with free surface. In-order to describe the mode dynamics for this structure, we need to estimate the values of τ_i^m. The values of τ_i^m for structures with free surface is, in general, different from the bulk case. The presence of surfaces modifies the phonon spectrum and its dynamics. The surface effect on the phonon dynamics is, often, described using a phenomenological relation for the surface scattering term. Here, we will use the underlying inter-atomic potential and a stochastic sampling approach to capture the surface effect on the phonon dynamics.

13

We shall use Eq.(27) to determine τ_i^m for the finite sized structure of interest. The unknowns in Eq.(27) are the terms on the L.H.S and the value of τ_i^n. We already parametrized τ_i^n as a function of ω_i using a reference bulk structure and, hence, is known. For estimating the term on the L.H.S of Eq.(27), we recognize that an ensemble averaging is required. We, therefore, need to generate ensembles of micro-states. For this purpose we will use a stochastic sampling approach. The details of the stochastic sampling approach are discussed in the Appendix B. Here, we briefly outline the main steps.

In the stochastic sampling method, we generate different samples of the mode variables a_i with a given PDF. The PDF for a_i is obtained using the QHM approximation and is given using Eq(2). Using this PDF, different instances of a_i are generated. The a_i values are, then, transformed to obtain the per-atom displacement. For each sampled set of a_i values, an atomic configuration is, thus, obtained. For the given atomic configuration the per atom forces are computed using the underlying inter-atomic potential. These are used to compute the mode force f_i. The L.H.S of Eq.(27) is, then, determined as

$$< (f_i + m\omega_i^2 a_i)^2 >= \frac{1}{n_{\text{ensb}}} \sum_{j=1}^{n_{\text{ensb}}} [(f_i + m\omega_i^2 a_i)^2]_j \tag{28}$$

Here, n_{ensb} is the number of samples in the canonical ensemble considered and $[...]_j$ is the value of the enclosed variable for the jth sample. Eq.(27) is, then, used to compute τ_i^m. This completes the parametrization step for the Langevin simulation. We will, now, use the Langevin dynamics to study the stress relaxation behavior.

We integrate the Langevin Eq. for each of the mode. We get a time series data of $a_i(t)$ and $v_i(t)$. The energy, $E_i(t)$, for a mode i is estimated as

$$E_i(t) = \frac{1}{2}m\omega_i^2 a_i^2 + \frac{1}{2}mv_i^2 \tag{29}$$

The modes satisfy equipartition of energy, this implies that $< E_i >= k_b T$. Hence, $\Delta E_i(t) = E_i(t) - k_b T$. We, now, use the Green-Kubo formulation and determine the non-equilibrium stress relaxation rate from the auto-correlation of equilibrium fluctuations. The stress component, σ_{ij}', is computed as $\sigma_{ij}' = \sum_{k=1}^{nmodes} \Delta E_k \Delta \lambda_k^{ij}$. We construct the stress auto correlation function, $C_{\sigma_{ij}'\sigma_{ij}'}(t)$, such that

$$C_{\sigma_{ij}'\sigma_{ij}'}(t) =< \sigma_{ij}'(0)\sigma_{ij}'(t) > \tag{30}$$

$C_{\sigma_{ij}'\sigma_{ij}'}(t)$ shows a decaying exponential behavior. From the decay rate of $C_{\sigma_{ij}'\sigma_{ij}'}(t)$ the stress relaxation rate, τ_{relax} is determined.

III. RESULTS AND DISCUSSION

We, first, consider the case of a bulk Ni structure and study the dissipation rate as a function of frequency under uni-axial deformation. Morse potential[36] is used to model the force field. Frequency values in the GHz range are considered. The dissipation rate is computed using non-equilibrium MD for comparing the results obtained using the multi-scale method. Here, we provide a brief description of the MD simulation set-up. All MD simulations were performed using the open source software LAMMPS[37].

The structure is first equilibrated at a desired temperature of 300 K. It is, then, decoupled from the thermostat. The structure is periodically deformed along the x direction and is evolved as a micro-canonical ensemble. The work done on the system results in an increase in the internal energy. From the rate of increase of internal energy per-unit period, the dissipation rate, E_{dissip}, is computed. We considered 5 ensembles for each frequency of operation. For each ensemble 100 oscillation periods were taken.

For estimating the dissipation rate using the multi-scale method we need to compute the different parameters in the constitutive relation. We, first, determine the components of the dissipation tensor, $\mathbf{D}$, for the bulk structure. For uni-axial deformation along the x direction, the only required value is the D_{1111}. We determined the value of D_{1111} using the QHM method. This requires computing λ_i^{11} for all the modes. Using the λ_i^{11} values in Eq.(17), D_{1111} is estimated to be 1.365 GPA at 300 K.

We also determined D_{1111} using the non-equilibrium stochastic sampling method. Using this method, the dissipative component of the stress tensor, σ_{ij}^D, is obtained for different values of ϵ_{11}. Figure 2 shows the variation of σ_{11}^D vs ϵ_{11}. The slope of this curve gives D_{1111} and is determined to be 1.37 GPA. This is in agreement with the value of D_{1111} computed using the QHM method. Figure 2, also, shows the variation of σ_{22}^D vs ϵ_{11}. The negative slope of this curve corresponds to a negative value of D_{1122}. The value of D_{1122} will be used, later, in computing the dissipation for the case of bi-axial deformation.

We, also, need to estimate the stress relaxation rate, τ_{relax}. For this purpose, we obtain the mode relaxation time, τ_i^m, using MD. The mode frequencies, ω_i, are determined using the QHM method. Using these values as input, mode Langevin dynamics is performed. The stress auto-correlation function, $C_{\sigma'_{11}\sigma'_{11}}(t)$ is computed using Eq.(30). From the decay of $C_{\sigma'_{11}\sigma'_{11}}(t)$, τ_{relax} is estimated to be 2.07 ps.
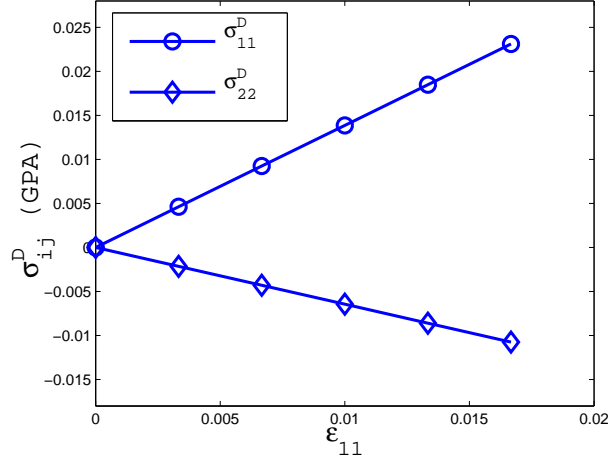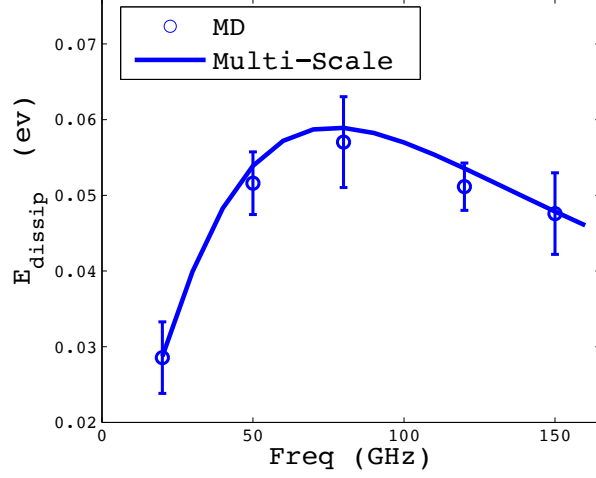
15

FIG. 2. The dissipative component of the stress, σ_{ij}^D, as a function of ϵ_{11}, obtained using the non-equilibrium stochastic sampling approach.

These parameters are, then, used to determine the time evolution of $\sigma_{11}^{'}$. We consider a spatially uniform strain field that varies sinusoidally in time such that $\epsilon_{11}(x,t) = \epsilon_0 sin(\omega_f t)$. Here, ϵ_0 is the strain amplitude and ω_f is the forcing frequency. The time evolution of $\sigma_{11}^{'}$ is obtained using Eq.(9). The dissipation rate, E_{dissip}, per unit period is, then, computed as
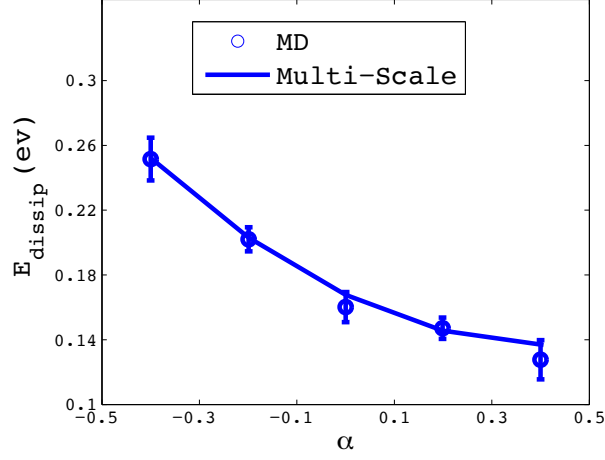
$$E_{\text{dissip}} = \int \int_0^{\frac{2\pi}{\omega_f}} \boldsymbol{\sigma}^{'} : \dot{\boldsymbol{\epsilon}} \, dt \, dV \tag{31}$$

Figure 3 a) shows the plot of E_{dissip} vs ω_f obtained using the multi-scale approach. The figure also shows the MD results. The two results are in good agreement with each other. The multi-scale approach, therefore, aptly describes the intrinsic dissipation in bulk solids.

We next consider the case of bi-axial deformation. The strain field for the bi-axial deformation is given as $\epsilon_{ij}(x,t) = \epsilon_0(\delta_{1i}\delta_{1j} + \alpha\delta_{2i}\delta_{2j})sin(\omega_f t)$. Here, α is the ratio of the strain in the y direction to that in the x direction. We consider different values of α for a fixed vibrational frequency of 40 GHz. Figure 3 b) shows the plot of E_{dissip} obtained for different values of α. We observe that E_{dissip} increases for negative values of α. This is because D_{1122} is negative. Further, there exists an optimum value of α for which E_{dissip} becomes minimum. Thus, by operating the resonator under such a desired strain state, the dissipation can be minimized. The negative sign of D_{1122} also suggests that it would be efficient to vibrate the structure under a dilation strain field. It would, also, be interesting to further explore the class of materials for which D_{1122} is positive. For such a material, an increase in dissipation

16

(a)

(b)

FIG. 3. (a) E_{dissip} as a function of the oscillation frequency, ω_f, for the case of bulk nickel structure. (b) E_{dissip} as a function of α for the bulk nickel structure forced under an oscillation frequency of 40 GHz.

with the increase in α value will be observed.

We, now, consider the case of structure with free surfaces. The structure has free surfaces along the y direction while it is periodic in the other two directions. A sinusoidal strain, $\epsilon_{11}(x,t) = \epsilon_0 sin(\omega_f t)$, is applied along the x direction. Here, ϵ_0 is the strain amplitude and ω_f is the oscillation frequency. Since the structure has free surfaces along the y direction, the applied strain also results in motion along the y direction. Using elasticity theory we shall,

17

first, obtain the displacement field along the y direction. The strain field, thus, obtained will be used as an input to compute the dissipation rate.

Let $u_y(y,t)$ denote the displacement field along the y direction. For a linear elastic solid with cubic symmetry, the stress component, $\sigma_{22}(y)$, is given as

$$\sigma_{22}(y) = C_{11}\frac{\partial v}{\partial y} + C_{12}\epsilon_0 sin(\omega_f t) \tag{32}$$

Here, C_{11} and C_{12} are the elastic constants. Using the expression for σ_{22} in the momentum balance Eq. we obtain

$$\frac{\partial^2 v}{\partial t^2} = C_{11}\frac{\partial^2 v}{\partial y^2} \tag{33}$$

Further, we also have the boundary conditions as $\sigma_{22}(0) = \sigma_{22}(L) = 0$, where L is the transverse length of the structure. The above Eq. admits a solution of the form $u_y(y,t) = (Asin(ky) + Bcos(ky))sin(\omega_f t)$ where $k = \omega_f\sqrt{\frac{\rho}{C_{11}}}$. The constants A and B are obtained using the boundary condition. The displacement field, $u_y(y,t)$, is, then, given as

$$u_y(y,t) = -\frac{C_{11}}{C_{22}}\frac{\epsilon_0}{k}\left(sin(ky) + \frac{cos(kl)-1}{sin(kl)}cos(ky)\right)sin(\omega_f t) \tag{34}$$

Here, k is the wave number. For the frequency range and the dimensions of the structure considered, the strain field in Eq.(34) is nearly uniform. The average strain, $\epsilon_{22}(t)$, in the y direction is, then, obtained as $\epsilon_{22}(t) = \frac{u_y(L,t)-u_y(0,t)}{L}$. Using the expression for $u_y(y,t)$ we get
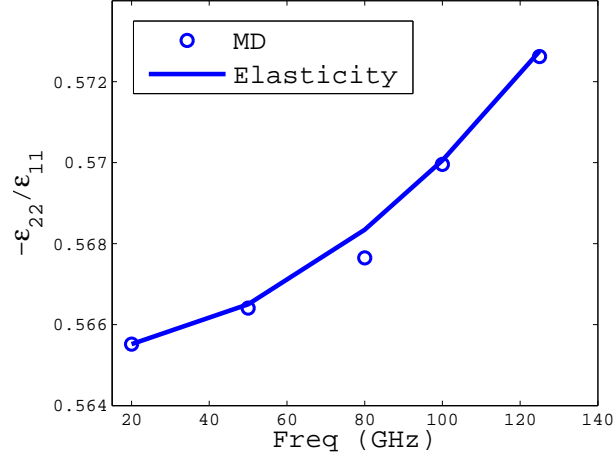
$$\epsilon_{22}(t) = -\frac{C_{12}}{C_{11}}\frac{tan(kl/2)}{kl/2}\epsilon_{11}(t) \tag{35}$$

The value of ϵ_{22} will be used to compute dissipation for structures with free surfaces.
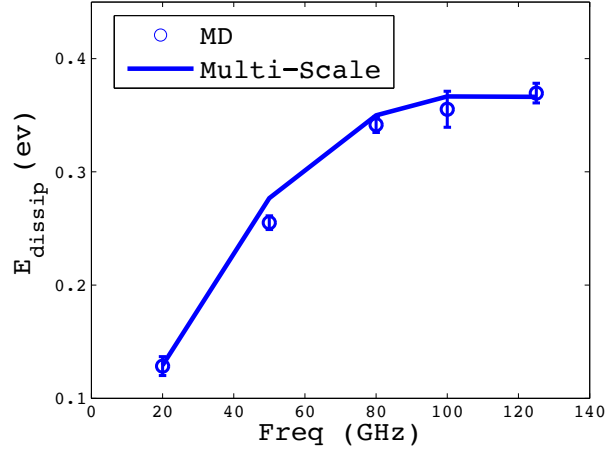
We consider a structure with a dimension of $10lc \times 8lc \times 10lc$ and with free surfaces along the y direction. Here, lc is the lattice constant. The strain field is a bi-axial strain field given as $\epsilon_{ij}(t) = (\delta_{i1}\delta_{j1}\epsilon_{11} + \delta_{i2}\delta_{j2}\epsilon_{22})sin(\omega_f t)$. Here, ϵ_{22} is related to ϵ_{11} using Eq.(35). Figure 4a) shows the plot of the ratio $\epsilon_{22}/\epsilon_{11}$ as a function of ω_f for this structure. The plot shows, that, the ratio increases with the increase in ω_f. The values are in good agreement with MD. We, shall, now use these strain values to compute dissipation using the multi-scale method.

For performing the multi-scale analysis for this structure, different parameters are determined. The value of τ_{relax} is estimated to be 1.45 ps. The strain field is plugged in the constitutive relation in Eq.(9) to obtain $\boldsymbol{\sigma}'(t)$. E_{dissip} is, then, computed using Eq(31). Figure 4b) shows the plot of E_{dissip} vs. ω_f. A non-monotonic behavior is observed. We also observed a non-monotonic behavior for the bulk structure. However, the frequency value

18

corresponding to the maximum value of E_{dissip} shifts to a higher value for the free surface case. This is because the stress relaxation time decreases because of the surface scattering. This, effectively, increases the value of ω_f corresponding to the maximum value of E_{dissip}.

(a)

(b)

FIG. 4. (a)The ratio $-\epsilon_{22}/\epsilon_{11}$ as a function of ω_f for a Ni structure with free surface. The structure has dimensions of $10lc \times 8lc \times 10lc$. Here, lc is the lattice unit. (b) E_{dissip} as a function of ω_f for the same structure.

We, next, studied the scaling of E_{dissip} with size. For this purpose, the length along the free surface (y) direction was varied, the other dimensions were kept constant. For each of the size D_{1111} and D_{1122} were obtained using the non-equilibrium sampling method. Figure

19

5 shows the plot of D_{1111} and D_{1122} as function of size.

We, then, computed τ_{relax} as a function of size. The τ_{relax} value for a structure with a lateral dimension L is given as

$$\frac{1}{\tau_{relax}} = \frac{1}{\tau_b} + \frac{L_0}{L\tau_s} \tag{36}$$

Here, v_g is the phonon velocity, τ_b is stress relaxation rate for the bulk structure and τ_s is the surface scattering rate for a reference structure with a lateral dimension L_0. τ_b was obtained for the case of bulk structure. We, also, determined τ_{relax} for a structure with free surface and with dimension L_0 using the mode Langevin dynamics. The value of τ_{relax} is used to parametrize τ_s. We, then, use Eq.(36) to determine τ_{relax} for a structure with any given lateral dimension L.
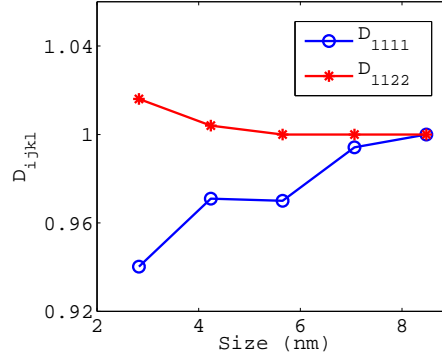

FIG. 5. The components of the dissipation tensor, $\mathbf{D}$, as a function of size. The values have been normalized with respect to the bulk value.

The different parameters, thus, obtained are used to compute E_{dissip} as a function of size. Figure 6 shows the plot E_{dissip} as a function of L and as obtained using the multi-scale theory. The MD values are also plotted alongside. The plot shows that E_{dissip} decreases with the decrease in size. This can be understood, predominantly, from the effect of surface on τ_{relax}. The surface scattering of phonon reduces τ_{relax}. The faster relaxation of the non-equilibrium stress implies weaker deviation from the equilibrium condition. Dissipation is governed by the deviation from the equilibrium path. Hence, E_{dissip}, decreases with the decrease in τ_{relax}.

It would be useful, here, to compare the effeciency of the multi-scale method with non-equilibrium MD. The limiting step for the proposed methodology is the determination of the mode eigen-vectors. For the structures considered, the computation of the mode vectors
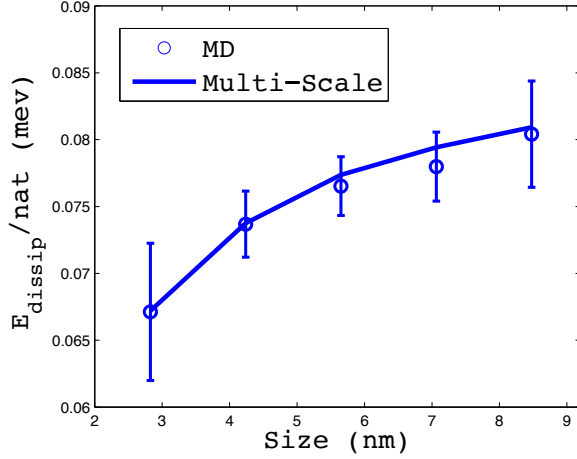
FIG. 6. E_{dissip} as a function of size for structures with free surface. The size denotes the lateral dimension, L, of the structure along the free surface direction. The dimension in the other two (periodic) directions are kept constant.

requires around 6 hours of CPU time. In comparison, a single trajectory of non-equilibrium MD run (of about 10 ns) takes around 36 CPU hours on the same machine. For a non-equilibrium MD simulation, the structure first needs to be equilibrated. Further, for a given frequency value one needs to consider a simulation time of 100 oscillation periods to get the steady state behavior. Multiple ensembles are needed to cancel out the effect of noise. Also, such simulations need to be carried out for different structures and for different frequencies of interest. In contrast, the method developed in this work just requires a single equilibrium MD trajectory of around 2 ns for the bulk structure. Also, the determination of relaxation rate for finite sized structure requires performing a mode space Langevin dynamics for only one structure. Using the dissipation tensor and the relaxation rate, the dissipation rate can, then, be obtained for a whole range of frequencies and different deformation states in a matter of few seconds.

IV. CONCLUSIONS

A multi-scale approach to model intrinsic dissipation under high frequency vibrations in a solid was developed. A non-equilibrium stress, that characterizes the deviation of the phonon distribution from the equilibrium state, was obtained. A constitutive equation that governs

the time evolution of the stress tensor was derived. The different parameters in the model were characterized using the QHM method and a stochastic sampling approach. Langevin dynamics in the mode space was used to obtain the stress relaxation. We studied dissipation in the frequency range of few GHz. Using the proposed formulation, the dissipation rate was computed for different cases. The results were compared with those obtained using non-equilibrium MD.

Appendix A: Non-equilibrium PDF

We derive an expression for the non-equilibrium PDF using the principle of maximum entropy[34,35]. We consider a collection of $ndof$ harmonic oscillators. Let a_i and v_i denote the displacement and velocity of the ith oscillator. The energy, E_i, for an oscillator i is given as $E_i = \frac{1}{2}ma_i^2\omega_i^2 + \frac{1}{2}mv_i^2$. Here m is the mass and ω_i denotes the frequency.

We have the following constraints on the system. The mean energy, $< E_n >$, of an oscillator n is given as $< E_n >= k_bT_n$. Here, T_n provides a measure of the temperature of the nth oscillator in the non-equilibrium state. We, then, seek to obtain the probability to observe a micro-state i. The PDF is obtained such that the entropy of the system is maximized subject to the imposed constraint. Let A denote the set of the displacement and V denote the set of velocity for all the oscillators for a given micro-state i. Let $P(A, V)$ denote the probability to observe this micro-state. The entropy, S, of the system is then given as

$$S = -\int P(A, V)logP(A, V)dAdV \tag{A1}$$

The constraint on the mean energy for the nth oscillator is given as

$$\int P(A, V)(\frac{1}{2}m\omega_n^2a_n^2 + \frac{1}{2}mv_n^2)dAdV = k_bT_n \tag{A2}$$

We, also, have the normalization constraint as

$$\int P(A, V)dAdV = 1 \tag{A3}$$

Taking these $ndof + 1$ constraints into account, the extremum problem for the PDF that maximizes the entropy can be stated as

$$\sup_P -\int \left(P(A, V)logP(A, V) + \alpha P + \sum_{n=1}^{ndof} \beta_n(\frac{1}{2}m\omega_n^2a_n^2 + \frac{1}{2}mv_n^2)P \right) dAdV \tag{A4}$$

Here, α and β_n are the Lagrange multipliers for enforcing the constraints. Taking the variation of the above Eq. with respect to P we obtain

$$P(A,V) = \frac{1}{Z} \prod_{n=1}^{ndof} exp\left(-\frac{\frac{1}{2}m\omega_n^2 a_n^2 + \frac{1}{2}mv_n^2}{k_b T_n}\right) \tag{A5}$$

Here, Z is the partition function that normalizes P. We, thus, obtain the PDF for the non-equilibrium state using the maximum entropy principle. We use this PDF to sample the non-equilibrium state and compute the dissipative stress component, σ_{ij}^D.

Appendix B: Stochastic Sampling

The objective of the stochastic sampling approach is to generate the micro-states from a given PDF. For the case of crystalline solids, the PDF is given as a Gaussian function. Using a Gaussian random number generator, the mircostates of a crystalline solid can, therefore, be generated. We will now discuss the details of this algorithm pertaining to our case.

The method requires as an input the mean position of the atoms, the mode eigen-vectors, $\mathbf{e}_i$ and the frequency ω_i. For a perfectly crystalline solid, the mean position of the atoms are generated using the underlying lattice structure. Ni at 300 K has a fcc crystalline structure and was used for our case. Using the mean atomic position the QHM analysis is performed. We, thus, obtain the values of ω_i and $\mathbf{e}_i$. We, next, construct the PDF, $P(a_i)$ for the mode co-ordinates, a_i. For the equilibrium state, $P(a_i)$, is given using Eq.(2). For the non-equilibrium state, additional constrains in terms of the mode temperature, T_i, are specified. $P(a_i)$ for such a case is given using Eq.(3). We recognize that the PDF for a_i, for either the equilibrium or the non-equilibrium state, are Gaussian functions. Using an algorithm to generate Gaussian random number, different instances of a_i can be obtained. We use the Box-Muller algorithm, and as implemented in the GNU package[38], for our purpose. We, thus, obtain different samples of a_i. For each samples of the a_i values we determine the per atom displacement. Let u_i^j denote the displacement for an atom i along the direction j. u_i^j is obtained from a_n using the linear transformation given as

$$u_i^j = \sum_{n=1}^{nmodes} a_n (e_n)_i^j \tag{B1}$$

Here, $(e_n)_i^j$ are the components of the eigen-vector $\mathbf{e}_n$ for an atom i along the direction j.

For each sample of a_n values, an atomic configuration is thus obtained. The configurations are, then, used to compute the ensemble averages of the required quantities.

---

* Corresponding author, electronic mail: aluru@illinois.edu

[1] B. Lassagne, D. Garcia-Sanchez, A. Aguasca and A. Bachtold, Nano Lett. **8**, 3735 (2008).

[2] K. Jensen, K. Kim and A. Zettl, Nature Nanotech. **3**, 1038 (2008).

[3] A. Naik, M. Hanay, W. Hiebert, X. Feng, M. Roukes, Nature Nanotech. **7**, 445 (2009)

[4] M. S. Hanay, S. Kelber, A. K. Naik, D. Chi, S. Hentz, E. C. Bullard, E. Colinet, L. Duraffourg and M. L. Roukes, Nature Naotech. **7**, 602 (2012).

[5] B. Ilic, Y. Yang, K. Aubin, R. Reichenbach, S. Krylov and H. G. Craighead, Nano Lett. **5**, 925 (2005).

[6] G. Zolfagharkhani, A. Gaidarzhy, P. Degiovanni, S. Kettemann, P. Fulde and P. Mohanty, Nature Nanotech. **12**, 720 (2008).

[7] L. G. Villanueva, R. B. Karabalin, M. H. Matheny, D. Chi, J. E. Sader and M. L. Roukes, Phys. Rev. B **87**. 024304 (2013).

[8] A. D. O'Connell, M. Hofheinz, M. Ansmann, R. C. Bialczak, M. Lenander, E. Lucero, M. Neeley, D. Sank, H. Wang, M. Weides, J. Wenner, J. M. Martinis and A. N. Cleland, Nature **464**, 697 (2010).

[9] K. L. Ekinci, Y. T. Tang and M. L. Roukes, J. Appl. Phys. **95**, 2682 (2004).

[10] J. Rieger, A. Isacsson, M. J. Seitner, J. P. Kotthaus and E. M. Weig, Nature Comm. **5**, 3345 (2014).

[11] G. D. Cole, I. W-Rae, K. Werbach, M. R. Vanner and M. Aspelmeyer, Nature Comm. **2**, 231 (2011).

[12] J. H. Ko, J. Jeong, J. Choi and M. Cho, Appl. Phys. Lett. **98**, 171909 (2011).

[13] S. Chakram, Y. S. Patil, L. Chang and M. Vengalattore, Phys. Rev. Lett. **112**, 127201 (2014).

[14] R. B. Bhiladvala and Z. J. Wang, Phys. Rev. E **69**, 036307 (2004).

[15] E. A. Ilin, J. Kehrbusch, B. Radzio, and E. Oesterschulze , J. Appl. Phys. **109**, 033519 (2011).

[16] R. Lifshitz and M. L. Roukes, Phys. Rev. B **61**, 5600 (2000).

[17] S. K. De and N. R. Aluru, Phys. Rev. B **74**, 144305 (2006).

[18] R. Lifshitz, Physica B **316**, 397 (2002).

[19] A. A. Kiselev and G. J. Iafrate, Phys. Rev. B **77**, 205436 (2008).

[20] K. Kunal and N. R. Aluru, Phys. Rev. B **84**, 245450 (2011).

[21] A. Croy, D. Midtvedt, A. Isacsson and J. M. Kinaret, Phys. Rev. B **86**, 235435 (2012).

[22] K. Kunal and N. R. Aluru, Nanotechnology **27**, 275701 (2013).

[23] K. Kunal and N. R. Aluru, J. Appl. Phys. **114**, 084302 (2013).

[24] D. Midtvedt, A. Croy, A. Isacsson, Z. Qi and H. S. Park, Phys. Rev. Lett. **112**, 145503 (2014).

[25] G. Palasantzas, J. Appl. Phys. **103**, 046106 (2008).

[26] C. Guthy, R. M. Das, B. Drobot, and S. Evoy, J. Appl. Phys. **108**, 014306 (2010).

[27] C. Seoanez, F. Guinea and A. H. Castro Neto, Phys. Rev. B **77**, 125107 (2008).

[28] L. G. Remus, M. P. Blencowe and Y. Tanaka, Phys. Rev. B **80**, 174103 (2009).

[29] J. W. Jiang, B. S. Wang, H. S. Park and T. Rabczuk, Nanotechnology, **25**, 025501 (2014).

[30] A. Akhiezer, J. Phys.(USSR) **1**, 289 (1939).

[31] H. E. Bommel and K. Dransfeld, Phys. Rev. **117**, 1245 (1960).

[32] Z. Tang, H. Zhao, G. Li and N. R. Aluru, Phys. Rev. B **74**, 064110 (2006).

[33] H. Zhao, Z. Tang, G. Li and N. R. Aluru, J. Appl. Phys. **96**, 064314 (2006).

[34] E. T. Jaynes, Phys. Rev. **106**, 620 (1957).

[35] Y. Kulkarni, K. Jaroslaw and M. Ortiz, J. Mech. and Phys. of Solids **56(4)** 1417 (2008).

[36] S. S. Mathur, Y. P. Sharma and P. N. Gupta, J. Appl. Phys. **42**, 5335 (1971).

[37] S. Plimpton, J. Comp. Phys. **117**, 1 (1995).

[38] G. Brian. GNU scientific library reference manual (Network Theory Ltd., 2009).